Journal of Earth Science, *Vol. 22*, *No. 2*, *p. 143–154*, *April 2011* *ISSN 1674-487X*
Printed in China
DOI: 10.1007/s12583-011-0166-9

Influences of Lower-Mantle Properties on the Formation of Asthenosphere in Oceanic Upper Mantle

David A Yuen
Department of Geology and Geophysics and Minnesota Supercomputing Institute, *University of Minnesota*, *Minneapolis*, *MN* 55415, *USA*
Nicola Tosi*
Department of Planetary Physics, *Institute of Planetary Research*, *German Aerospace Center* (*DLR*), *Berlin*, *Germany*
Ondrej Čadek
Department of Geophysics, *Faculty of Mathematics and Physics*, *Charles University*, *Prague*, *Czech Republic*

ABSTRACT: Asthenosphere is a venerable concept based on geological intuition of Reginald Daly nearly 100 years ago. There have been various explanations for the existence of the asthenosphere. The concept of a plume-fed asthenosphere has been around for a few years due to the ideas put forth by Yamamoto et al.. Using a two-dimensional Cartesian code based on finite-volume method, we have investigated the influences of lower-mantle physical properties on the formation of a low-viscosity zone in the oceanic upper mantle in regions close to a large mantle upwelling. The rheological law is Newtonian and depends on both temperature and depth. An extended-Boussinesq model is assumed for the energetics and the olivine to spinel, the spinel to perovskite and perovskite to post-perovskite (ppv) phase transitions are considered. We have compared the differences in the behavior of hot upwellings passing through the transition zone in the mid-mantle for a variety of models, starting with constant physical properties in the lower-mantle and culminating with complex models which have the post-perovskite phase transition and depth-dependent coefficient of thermal expansion and thermal conductivity. We found that the formation of the asthenosphere in the upper mantle in the vicinity of large upwellings is facilitated in models where both depth-dependent thermal expansivity and conductivity are included. Models with constant thermal expansivity and thermal conductivity do not produce a hot low-viscosity zone, resembling the asthenosphere. We have also studied the influences of a cylindrical model and found similar results as the Cartesian model with the important difference that upper-mantle temperatures were much cooler than the Cartesian model by about 600 to 700 K. Our findings argue for the potentially important role played by lower-mantle material properties on

This study was supported by the CMG Program of the National Science Foundation, the Senior Visiting Professorship Program of the Chinese Academy of Sciences, the Helmholtz Association through the Research Alliance "Planetary Evolution and Life", and the European Commission through the Marie Curie Research Training Network c2c (No. MRTN-CT-2006-035957).
*Corresponding author: nic.tosi@googlemail.com

Manuscript received September 22, 2010.
Manuscript accepted December 28, 2010.

the development of a plume-fed asthenosphere in the oceanic upper mantle.

KEY WORDS: oceanic asthenosphere, lower mantle, thermal expansivity, thermal conductivity, phase transition.

INTRODUCTION

Asthenosphere is uniquely linked to the mobility and stability of plate motions and long-wavelength mantle circulation in the planet earth (e.g., Richards et al., 2001). The notion of an asthenosphere in geodynamics was advanced nearly one century ago by Daly (1914) in his pursuit of linking surface geological observations with physical properties of rocks under pressure. It hinges on the notion of a soft layer underneath the crust. How is this soft zone produced? van Bemmelen and Berlage (1934) found evidence of such a soft layer underneath Fennoscandia from relaxation curves of beaches due to post-glacial uplift. Elsasser (1969) explained the temporal evolution of earthquake aftershocks by using a stress-diffusion model in which the asthenosphere serves as a means to link the timescales of the order of a few to tens of years from large Alaskan earthquakes. There have been attempts to link the asthenosphere to partial melting (Bottinga and Allegre, 1973; Oldenbur and Brune, 1972), hydrogen enrichment and its consequences on the properties of mantle rocks (Karato, 2008, 1986) and thermal-mechanical coupling from boundary-layer mantle flows (Schubert et al., 1976). Mantle upwelling and decompression melting beneath oceanic ridges may have important consequences for the development of convective flows as the lithosphere ages (e.g., Parmentier, 2007). Recently Yamamoto et al. (2007) argued that regional asthenosphere under oceans can be formed dynamically by focused upwellings in the upper mantle.

In this article, we show with a two-dimensional Cartesian mantle convection model the importance of lower-mantle depth-dependent properties in producing scenarios in which an oceanic asthenosphere of regional extent can be formed from upwellings in the upper mantle. We do not concern ourselves with asthenosphere formed under continental interiors (e.g., Dixon et al., 2004). We begin by introducing our model, first in the geophysical aspects and then the numerical framework. We then present the results in Cartesian geometry which will be reinforced by a simulation in a cylindrical geometry and follow with our conclusions and future projections.

MODEL DESCRIPTION

Rheology and Material Parameters

We have modeled mantle flow in an aspect-ratio 10, 2-D Cartesian box for an isochemical creeping fluid heated solely from below with Newtonian viscosity, depth-dependent thermal expansivity and conductivity and multiple phase transitions. We have used the so-called extended Boussinesq approximation (e.g., Schubert et al., 2001) which differs from the well-known Boussinesq approximation in that the effects of adiabatic compression and viscous dissipation are included in the equation for the energy conservation while the flow is still considered as incompressible, i.e. the density is kept constant except at the phase transitions. All the details concerning the way the equations are non-dimensionalized and the parameters used can be found in Tosi et al. (2010) to which the reader is referred for a more thorough description of the elliptic momentum equation and the non-linear parabolic temperature equation, with viscous and adiabatic heatings and latent-heat effects from phase transitions included.

The dimensionless viscosity η depends on pressure (depth) and temperature as follows (e.g., Matyska and Yuen, 2007)

$$\eta(z,T) = \eta_1(z)\min\left[f, \max\left[f^{-1}, \eta_2(T)\right]\right] \qquad (1)$$

The depth is given by z and temperature by T. The depth-dependent part is defined as in Hanyk et al. (1995)

$$\eta_1(z) = \left(1 + 214.3z\exp\left(-16.7\left(0.7 - z\right)^2\right)\right) \qquad (2)$$

Equation (2) implies a viscosity maximum in the mid-lower mantle (blue line in Fig. 1) which is consistent with inversions of the long-wavelength geoid (Čadek and van den Berg, 1998; Ricard and Bai, 1991) and of observables related to post-glacial rebound (Tosi et al., 2005; Mitrovica and Forte, 2004; Forte and Mitrovica, 2001). An activation volume is implicit in equation (2) and is lower than 5 cm^3/mol throughout the mantle but it has a non-monotonic

character (Wentzcovich et al., 2009). The temperature-dependent portion takes the form of an Arrhenius-type rheological law (Davies, 1999)

$$\eta_2(T) = \exp\left(10\left(\frac{0.6}{0.2+T} - 1\right)\right) \quad (3)$$

The factor f in equation (1) limits the viscosity variations due to temperature between f^1 and f. In this study, f is used as a parameter which can take values of 10, 50 or 100 corresponding to maximum viscosity variations due to temperature of a factor of 100, 2 500 and 10 000, respectively, with the latter value representing somewhat an upper limit to guarantee the mobility of the top thermal boundary layer and prevent the formation of a stagnant lid (Moresi and Solomatov, 1995). While truncating the large viscosity variations associated with equation (3) can affect the calculations of the surface stresses, the influence of the truncation on the heat transport and mean flow velocities is of lesser importance (King, 2009). To obtain the dimensional viscosity field shown in Figs. 4, 5 and 6, a reference value of 10^{22} Pa·s has been chosen.

The thermal expansivity α is either considered constant or dependent on depth according to the profile shown in Fig. 1 by the red line. This implies an overall decrease of α by about one order of magnitude

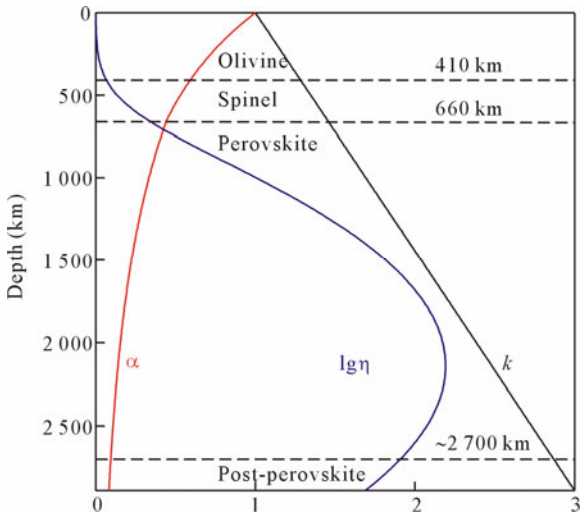

Figure 1. Schematic diagram of the physical model. The non-dimensional depth profiles of thermal expansivity (red line), thermal conductivity (black line) and logarithm of the pressure-dependent part of viscosity (blue line), as well as the three phase transitions (dashed lines), are shown.

throughout the mantle in such a way that the Anderson-Grüneisen parameter is approximately 5 for the upper mantle and 7 for the lower mantle, consistently with estimates for olivine (Chopelas and Boehler, 1992) and with the latest high-pressure measurements of perovskite volume by X-ray diffraction (Katsura et al., 2009).

Although in a fully consistent thermodynamics framework the thermal conductivity is related to the density and thermal expansivity via an appropriate equation of state (Nakagawa et al., 2010; Wentzcovitch et al., 2010; Yu et al., 2008; Poirier, 1991), here, for simplicity, the thermal conductivity k is considered to be either constant or linearly dependent on depth as shown in Fig. 1 by the black line. According to this profile, k is assumed to increase by a factor of 3 across the mantle, implying a thermal conductivity of about 10 W/mK near the core-mantle boundary (CMB). Although no conclusive agreement has been reached on the exact values that the total lattice thermal conductivity takes at lower-mantle pressures, growing consensus supported by experiments and theoretical first-principle calculations favors a picture of k increasing across both the upper (e.g., Xu et al., 2004) and lower mantle (e.g., Goncharov et al., 2010) with values at the CMB ranging from 6 W/mK (de Koker, 2010) to about 10 W/mK (Goncharov et al., 2010; Ohta, 2010; Tang and Dong, 2010) to even 20–30 W/mK (Hofmeister, 2008).

All three major phase transitions are taken into account in our models (see Fig. 1), namely from olivine to spinel at 410 km depth (Clapeyron slope γ=3 MPa/K (Bina and Helffrich, 1994), density jump $\delta\rho$=273 kg/m^3 (Steinbach and Yuen, 1995)), from spinel to perovskite (γ=-2.5 MPa/K (Bina and Helffrich, 1994), $\delta\rho$=342 kg/m^3 (Steinbach and Yuen, 1995)) and from perovskite to post-perovskite (ppv) according to local conditions of temperature and pressure (γ=13 MPa/K (Tateno et al., 2009), $\delta\rho$=67.5 kg/m^3 (Oganov and Ono, 2004)). Phase transitions are parameterized in a standard way by means of a hyperbolic phase-function (Richter, 1973) using a phase loop of 20 km width. To model the transition to the ppv phase we have used a temperature intercept of the Clapeyron curve at the CMB of 3 600 K. Such a temperature is lower than our assumed CMB

temperature of 3 800 K (Kawai and Tsuchiya, 2009). Under these conditions ppv forms only locally, generally beneath cold downwellings where the local geotherm is crossed twice by the Clapeyron curve which gives rise to the so called "double-crossing" (Hernlund et al., 2005), i.e. to ppv lenses underlain by a thin layer of perovskite. Although the current knowledge of the rheology of ppv is still very uncertain (Karato, 2010; Yamazaki and Karato, 2007), recent experiments (e.g., Hunt et al., 2009; Yoshino and Yamazaki, 2007) and first-principles calculations (Ammann et al., 2010) indicate that ppv might be significantly weaker than perovskite, albeit extremely anisotropic (Ammann et al., 2010; Walte et al., 2009). Therefore, in our models we have assumed the viscosity of ppv be lower than that of the surrounding perovskite by one order of magnitude. Furthermore, we have also assumed for ppv a thermal conductivity by a factor of 2 larger than that of its surroundings (Ohta, 2010; Hofmeister, 2007; Oganov and Ono, 2005).

Numerical Setup

Conservation equations are solved with the code YACC (Yet Another Convection Code) (King et al., 2010; Tosi et al., 2010) via a primitive-variable, 2nd order accurate finite-volume formulation that employs a semi-Lagrangian semi-implicit scheme to treat the advection and diffusion of the temperature (Spiegelman and Katz, 2006). Free-slip boundary conditions are used for the momentum equation, while isothermal top and bottom boundaries along with reflective side walls are employed to solve the thermal energy equation.

The system is heated solely from below, while internal heat sources are neglected. This is consistent with the assumption that Cartesian models tend to deliver mean temperatures that largely overestimate those found in more realistic spherical or cylindrical geometries (O'Farrell and Lowman, 2010).

As thermal initial condition, we have chosen an adiabatic profile with potential temperature of 1 600 K, boundary layers at the top and bottom and a 1% random perturbation. To discretize the model domain, we have used 1 000 equally spaced nodal points in the horizontal direction and 200 points in the vertical direction with refinement by a factor of 4 near the top and bottom thermal boundary layers.

The two linear systems arising from the discretization of the momentum and energy equations are solved using the OpenMP parallel direct solver PARDISO (Schenk et al., 2000).

We will also show one model run which has been conducted in a cylindrical geometry (see Fig. 6). For this we have employed the finite-volume cylindrical-spherical code GAIA (Huettig, 2008; Huettig and Stemmer, 2008) and used the same parameters and setting which were employed for the Cartesian models (apart from the reflecting boundary conditions at side walls in which a cylindrical geometry are not needed).

RESULTS

Global Temperature Fields

All the models presented in this work feature temperature- and depth-dependent viscosity and the upper-mantle phase transitions at depths of 410 and 660 km. We first display in Fig. 2 the long-term asymptotic temperature field for models without ppv. At the same time we vary the thermodynamic properties from a model in which these are constant (panel (a)) to models with depth-dependent thermal expansivity and conductivity (panels (b) and (c)). A viscosity variation of a factor of 2 500 (i.e. f=50 in equation (1)) due to temperature has been kept throughout. What is clear is the propensity for thicker plumes with a lot of spreading of hot material in the upper mantle with the addition of depth-dependent mantle properties as previously evidenced in earlier studies of mantle convection with depth-dependent thermal expansivity (e.g., Hansen et al., 1993; Leitch et al., 1991). From the average temperature profiles shown on the right we can also observe a remarkable flattening of the temperature gradient in the entire mantle due to adiabatic heating/cooling caused by the decrease of the thermal expansivity with depth. The differences between models with depth-dependent thermal expansivity only and models with both depth-dependent thermal expansivity and conductivity are minor apart from a slight increase in the mean mantle temperature (compare panels (b) and (c)) caused by more efficient heating of cold subducted material near the CMB due to the use of a large thermal conductivity at depth. Apart from a

slight increase in the average mantle temperature, we have also observed that models that feature a depth-dependent thermal conductivity and constant thermal expansivity (not shown here) do not exhibit a fundamentally different dynamics with respect to models with constant thermodynamic properties such as that shown in Fig. 2a. In particular, the thermal gradient induced by adiabatic compression remains unaltered.

Next in Fig. 3 we include the ppv transition. We find a general increase of mantle temperature (Matyska and Yuen, 2006; Nakagawa and Tackley, 2004) which becomes particularly evident when both depth-dependent thermal expansivity and conductivity are considered (Tosi et al., 2010). Such a temperature increase is caused by the presence of ppv which greatly enhances the instability of the bottom thermal boundary layer, promoting the formation of a larger number of upwellings (compare for instance Fig. 3a with Fig. 2a). The second box below the temperature field shows in the bottom 780 km of the mantle the occurrence of the ppv phase. The amount of ppv decreases sharply with the presence of depth-dependent thermal conductivity as a consequence of the dramatic increase of the mantle temperature. Furthermore, the

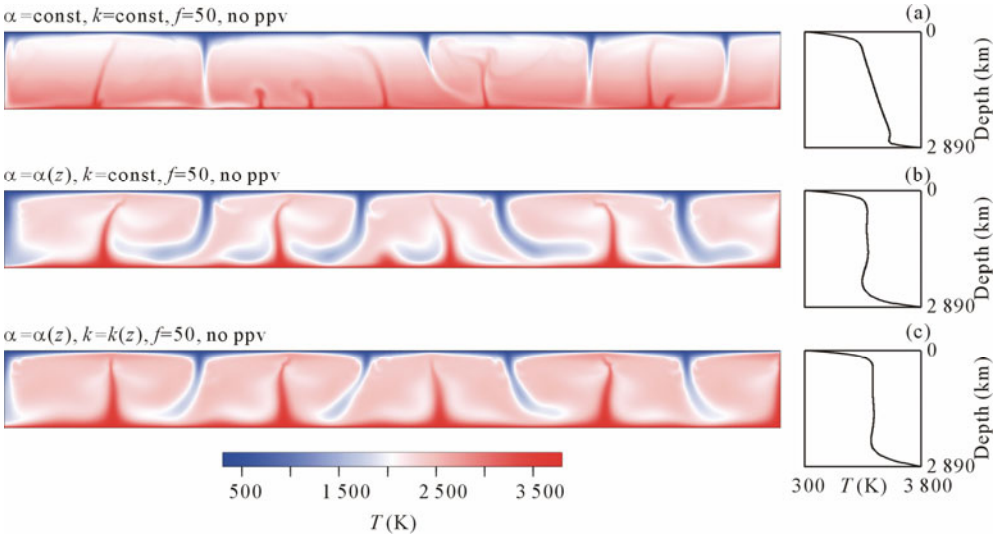

Figure 2. Effect of depth-dependent expansivity and conductivity on the global temperature field without post-perovskite. Long-term snapshots of the temperature (left) and corresponding average profiles (right).

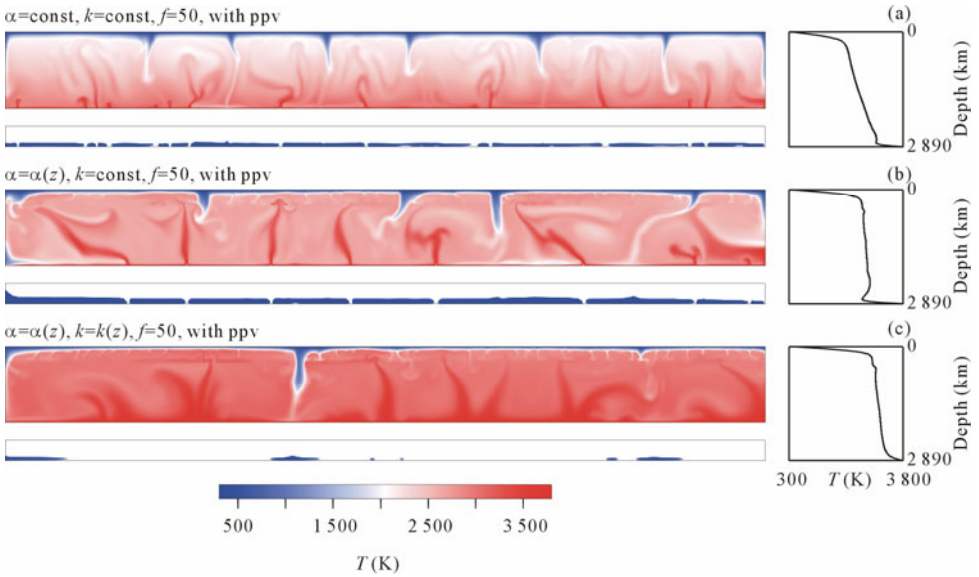

Figure 3. As in Fig. 2 but for models featuring the post-perovskite phase change. The occurrence of post-perovskite is shown below the temperature field in a box comprising the bottom 780 km of the domain.

figure illustrates the important role of depth-dependent thermal conductivity in promoting the formation of large-scale clusters of plumes (Tosi et al., 2010). We note that the upper-mantle temperatures produced in the Cartesian models because of the thermodynamic constraints would lead to large-scale melting in the upper mantle above 400 km depth. Therefore, we show below the impact from using a 2-D cylindrical model, which will reduce considerably the temperature in the upper mantle.

Zoomed-in Views

We take now a close-up view of the top 290 km of the mantle shown in Figs. 4 and 5 selected regions with aspect ratio 3 that portray the behavior of upwellings in the upper mantle which is characteristic of the model considered. In Fig. 4 are shown the velocity vectors and temperature field on the left and the logarithmic viscosity field on the right for a series of models without ppv. We can discern clearly the tendency of a low viscosity to form with depth-dependent properties by comparing panels (d) with (a). For the case with f=50 (panel (c)), the horizontal velocity vectors display a pronounced horizontal jet behavior which appears to be much more evident than in the constant property case (panel (a)) in which a nearly uniform horizontal upper-mantle flow is observed. Admittedly, these models do not have the proper plastic rheology for plate-like behavior in the top portion which would promote the formation of

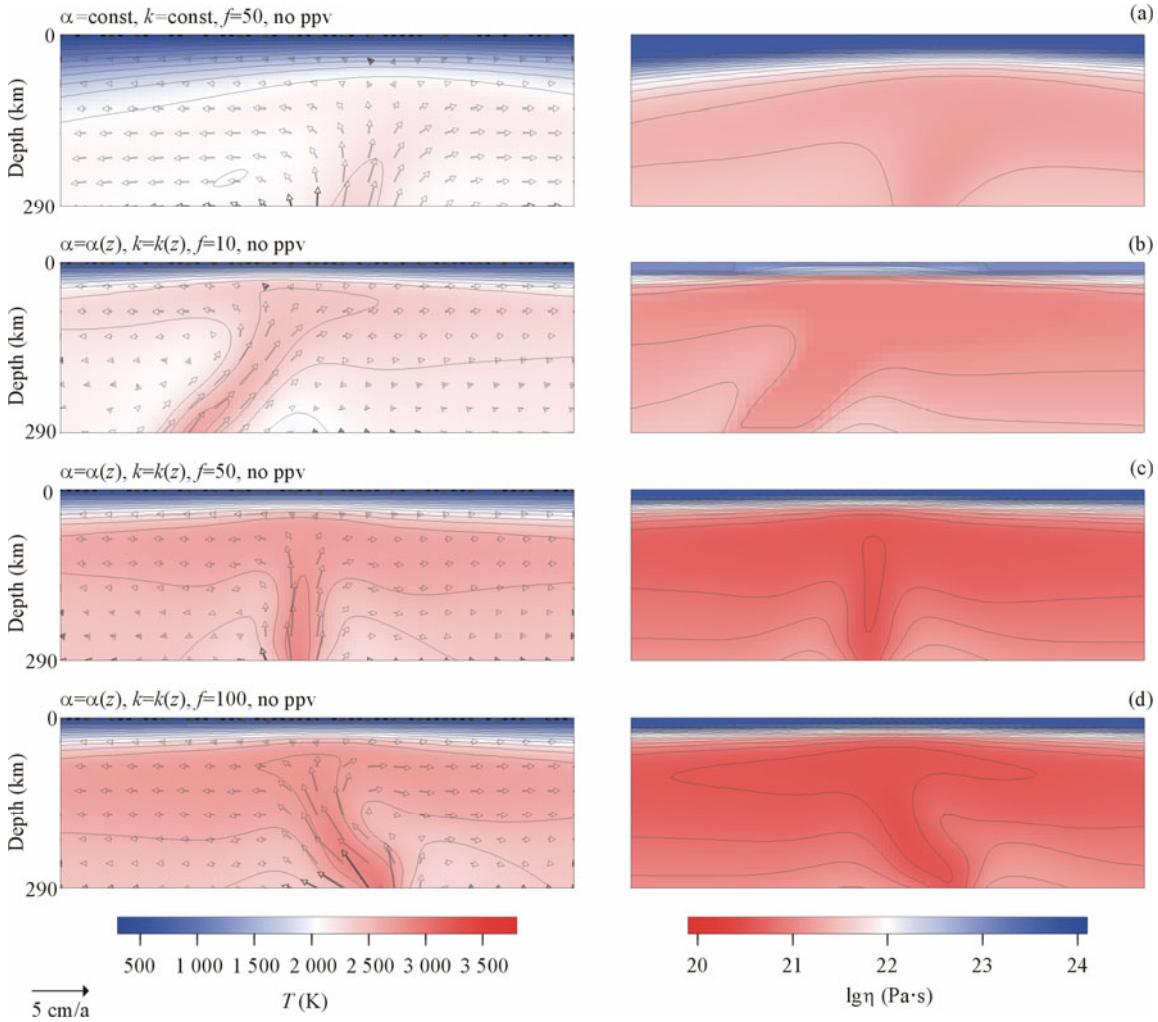

Figure 4. Zoomed-in shots of upper-mantle plumes. Effects of depth-dependent expansivity, conductivity and temperature viscosity contrast on the temperature (left column) and viscosity (right column) without post-perovskite. Over the temperature plots the direction and magnitude of flow velocities are also shown. The factor *f* which determines the viscosity variations due to temperature is varied between 10, 50 and 100, corresponding to an effective viscosity contrast of 100, 2 500 and 10 000, respectively.

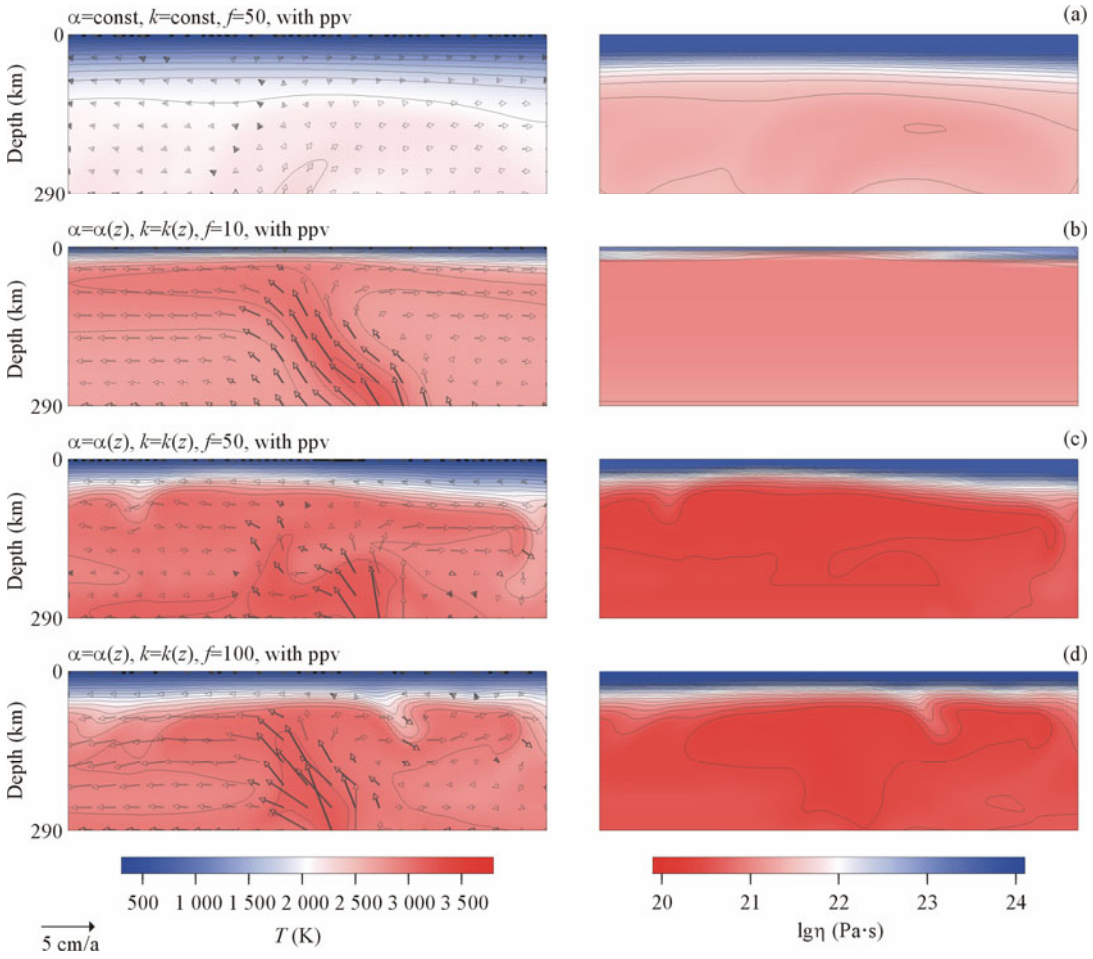

Figure 5. As in Fig. 4 but for model featuring the post-perovskite phase change.

low-viscosity zones. On the one hand, with respect to the model shown in panel (a), the reduction of the asthenospheric viscosity associated with the arrival of a plume in the presence of depth-dependent thermodynamic properties is only moderate for small temperature viscosity contrasts (panel (b)). On the other hand, it becomes much more pronounced when the factor f which governs the sensitivity of viscosity to variations of the temperature is raised to 50 or 100 (panels (c) and (d)).

Next in Fig. 5 we study the close-up situation in the presence of ppv. We observe that the small-scale instabilities that ppv induces near the CMB reflect in a small-scale convective motion in the uppermost mantle with a pronounced low-viscosity zone present when depth-dependent thermodynamic properties are considered in concert with relatively large viscosity contrasts due to temperature (see panels (c) and (d)). Again we clearly observe the effects from a well-focused upwelling, which is aided by the presence of depth-dependent properties. In particular, the velocity field in panel (c) characterizes a bent shaped plume which is first deflected horizontally in the transition zone and then reemerges vertically beneath the lithosphere (Yuen et al., 1996; Maruyama, 1994) in a fashion that resembles the sketch shown below in Fig. 7.

Finally, in Fig. 6 we show the effects of cylindrical geometry on reducing the upper-mantle temperatures while at the same time producing a more interesting dynamics because of the more realistic curvilinear geometry. We call attention to the drastic reduction in the upper-mantle temperature as compared to the Cartesian models in Figs. 2 and 3. The outline of the low-viscosity zone adjacent to upwellings can be discerned in the right panel. As the viscosity contour lines show, this is the region where the viscosity drop due to the arrival of a hot plume near the surface is the greatest. Nevertheless, the horizontal spreading of hot plume material is responsible for a global reduction of the asthenospheric viscosity which assumes greater

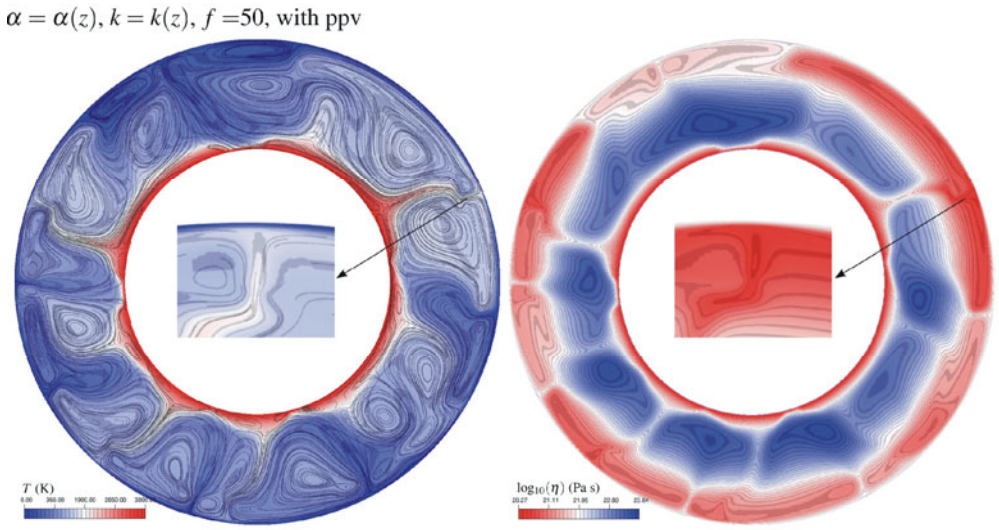

Figure 6. Temperature and streamlines (left) and viscosity (right) from a model run in cylindrical geometry performed with the code GAIA (Huettig, 2008; Huettig and Stemmer, 2008). Parameters are the same as those used in Fig. 5c. A zoomed-in view on a plume bent at the transition zone and emerging in the upper mantle is also shown. Note the dramatic reduction of temperature caused by the use of a cylindrical geometry. The largest value of the velocity field is 7.2 cm/a. Such a value is typically observed in the conduit of plumes passing through the transition zone such as that shown here in the zoomed-in view.

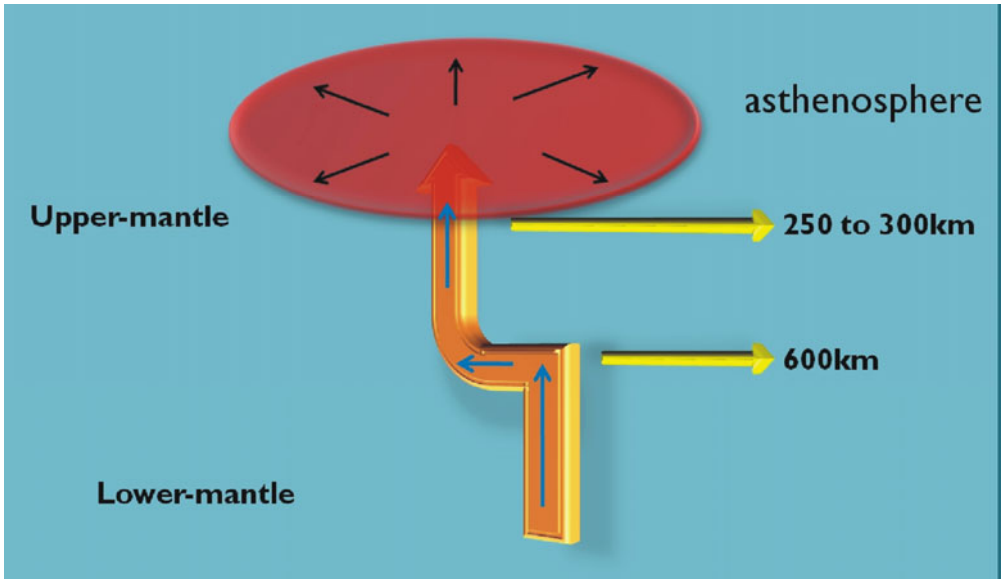

Figure 7. 3-D perspective of plume-fed asthenosphere model and bent-plume concept promulgated by Maruyama (1994) with a fast channel flow in the boundary between the upper and lower mantle.

values only near colder regions of downgoing flow. The streamlines on the left panel reveal the complex dynamics of this type of convection when cast in a cylindrical geometry, because of the increase in the degrees of freedom in the domain. We also note the bent plume formed at the 660 km discontinuity.

IMPLICATION OF A REGIONAL OCEANIC ASTHENOSPHERE AND FUTURE PERSPECTIVES

By using direct numerical simulation of 2-D mantle convection, we have shed some light on the potentially important role played by lower-mantle properties in the formation of a plume-fed asthenosphere in the shallow oceanic upper mantle. Recent

detailed seismic imaging work, using multiple reflected shear waves (Cao et al., 2010a), has also helped to unveil the bent plume structure in the neighborhood of Hawaiian Archipelago, which looks strikingly close to the schematic diagram depicted in Fig. 7 (Cao et al., 2010b). An earlier numerical simulation by Yuen et al. (1996) in 2-D axisymmetric geometry has shown this dynamical possibility of a bent plume with a channel flow character in the transition zone. Maruyama (1994) had already proposed such an elbow-shaped plume on geological and petrological grounds. Therefore, we need to investigate further this problem with high-resolution 2-D cylindrical model, and then follow up with a regional spherical model, using upwards of a billion regularly spaced grid points, and with variable viscosity in the mantle and also a plate-like rheology in the lithosphere in order to see whether a self-consistent generated thin asthenosphere can be produced. This thin structure with low viscosity would have important consequences on the style of mantle circulation (Stein and Hansen, 2008; Hoink and Lenardic, 2008). Additional work should also be carried out with continental lithosphere with greater thickness in concert with seismic imaging there. Another topic of interest would be the majorite transition associated with the pyroxene phase to see whether additional regional layering below the 660 km discontinuity can be formed from hot lower-mantle upwellings.

ACKNOWLEDGMENTS

We thank stimulating discussion with Jason Phipps-Morgan, Maarten de Hoop and Shigenori Maruyama. Comments by Masanori C Kameyama and an anonymous reviewer helped to improve an earlier version of this manuscript. Support of this research has come from CMG Program of the National Science Foundation, the Senior Visiting Professorship Program of the Chinese Academy of Sciences, the Helmholtz Association through the Research Alliance “Planetary Evolution and Life”, and the European Commission through the Marie Curie Research Training Network c2c (No. MRTN-CT-2006-035957).

REFERENCES CITED

Ammann, M. W., Brodholt, J. P., Wookey, J., et al., 2010. First-Principles Constraints on Diffusion in Lower Mantle Minerals and a Weak D” Layer. *Nature*, 465(7297): 462–465

Bina, C. R., Helffrich, G., 1994. Phase Transitions Clapeyron Slopes and Transition Zone Seismic Discontinuity Topography. *J. Geophys. Res.*, 99(B8): 15853–15860

Bottinga, Y., Allegre C. J., 1973. Thermal Aspects of Seafloor Spreading and the Nature of the Oceanic Crust. *Tectonophysics*, 18(1–2): 1–17

Čadek, O., van den Berg, A. P., 1998. Radial Profiles of Temperature and Viscosity in the Earth’s Mantle Inferred from the Geoid and Lateral Seismic Structure. *Earth Planet. Sci. Lett.*, 164(3–4): 607–615

Cao, Q., Wang, P., van der Hilst, R. D., et al., 2010a. Imaging the Upper Mantle Transition Zone with a Generalized Radon Transform of SS Precursors. *Phys. Earth Planet. Inter.*, 180(1–2): 80–91

Cao, Q., van der Hilst, R. D., de Hoop, M. V., et al., 2010b. Complex Plume Dynamics in the Transition Zone underneath the Hawaii Hotspot: Seismic Imaging Results. AGU Fall Meeting

Chopelas, A., Boehler, R., 1992. Thermal Expansivity in the Lower Mantle. *Geophys. Res. Lett.*, 19(19): 1983–1986

Daly, R. A., 1914. Igneous Rocks and Their Origin. McGraw-Hill, New York. 563

Davies, G. F., 1999. Dynamic Earth. Cambridge University Press, Cambridge. 458

de Koker, N., 2010. Thermal Conductivity of MgO Periclase at High Pressure: Implications for the D” Region. *Earth Planet. Sci. Lett.*, 292(3–4): 392–398

Dixon, J. E., Dixon, T. H., Bell, D. R., et al., 2004. Lateral Variation in Upper Mantle Viscosity: Role of Water. *Earth Planet. Sci. Lett.*, 222(2): 451–467

Elsasser, W. M., 1969. Convection and Stress Propagation in the Upper Mantle. In: Runcorn, S. K., ed., The Application of Modern Physics to the Earth and Planetary Interiors. Wiley, New York. 223–246

Forte, A. M., Mitrovica, J. X., 2001. Deep-Mantle High-Viscosity Flow and Thermochemical Structure Inferred from Seismic and Geodynamic Data. *Nature*, 410(6832): 1049–1056

Goncharov, A. F., Struzhkin, V. V., Montoya, J. A., et al., 2010. Effect of Composition, Structure, and Spin State on the Thermal Conductivity of the Earth’s Lower Mantle. *Phys. Earth Planet. Inter.*, 180(3–4): 148–153

Hansen, U., Yuen, D. A., Kroening, S. E., et al., 1993.

Dynamical Consequences of Depth-Dependent Thermal Expansivity and Viscosity on Mantle Circulations and Thermal Structure. *Phys. Earth Planet. Inter.*, 77(3–4): 205–223

Hanyk, L., Moser, J., Yuen, D. A., et al., 1995. Time-Domain Approach for the Transient Responses in Stratified Viscoelastic Earth Models. *Geophys. Res. Lett.*, 22(10): 1285–1288

Hernlund, J. W., Thomas, C., Tackley, P. J., 2005. A Doubling of the Post-Perovskite Phase Boundary and Structure of the Earth's Lowermost Mantle. *Nature*, 434(7035): 882–886

Hofmeister, A. M., 2007. Pressure Dependence of Thermal Transport Properties. *Proc. Natl. Acad. Sci.*, 104(22): 9192–9197

Hofmeister, A. M., 2008. Inference of High Thermal Transport in the Lower Mantle from Laser-Flash Experiments and the Damped Harmonic Oscillator Model. *Phys. Earth Planet. Inter.*, 170(3–4): 201–206

Hoink, T., Lenardic, A., 2008. Three-Dimensional Mantle Convection Simulations with a Low-Viscosity Asthenosphere and the Relationship between Heat Flow and the Horizontal Length Scale of Convection. *Geophys. Res. Lett.*, 35(10): L10304

Huettig, C., 2008. Scaling Laws for Internally Heated Mantle Convection: [Dissertation]. Westfaelischen Wilhelms-Universitaet, Muenster

Huettig, C., Stemmer, K., 2008. Finite Volume Discretization for Dynamic Viscosities on Voronoi Grids. *Phys. Earth Planet. Inter.*, 171(1–4): 137–146

Hunt, S. A., Weidner, D. J., Li, L., et al., 2009. Weakening of Calcium Iridate during Its Transformation from Perovskite to Post-Perovskite. *Nature Geosci.*, 2(11): 794–797

Karato, S. I., 1986. Does Partial Melting Reduce the Creep Strength of the Upper Mantle? *Nature*, 319(6051): 309–310

Karato, S. I., 2008. Insights into the Nature of Plume-Asthenosphere from Central Pacific Geophysical Anomalies. *Earth Planet. Sci. Lett.*, 274(1–2): 234–240

Karato, S. I., 2010. The Influence of Anisotropic Diffusion on the High-Temperature Creep of a Polycrystalline Aggregate. *Phys. Earth Planet. Inter.*, 183(3–4): 468–472

Katsura, T., Yokoshi, S., Kawabe, K., et al., 2009. *P-V-T* Relations of $MgSiO_3$ Perovskite Determined by In Situ X-Ray Diffraction Using a Large-Volume High-Pressure Apparatus. *Geophys. Res. Lett.*, 36: L01305

Kawai, K., Tsuchiya, T., 2009. Temperature Profile in the Lowermost Mantle from Seismological and Mineral Physics Joint Modeling. *Proc. Natl. Acad. Sci.*, 106(52): 22119–22123

King, S. D., 2009. On Topography and Geoid from 2-D Stagnant-Lid Convection Calculations. *Geochem., Geophys., Geosyst.*, 10: Q03002

King, S. D., Lee, C., Van-Keken, P. E., et al., 2010. A Community Benchmark for 2D Cartesian Compressible Convection in the Earth's Mantle. *Geophys. J. Int.*, 180(1): 73–87

Leitch, A. M., Yuen, D. A., Sewell, G., 1991. Mantle Convection with Internal Heating and Pressure-Dependent Thermal Expansivity. *Earth Planet. Sci. Lett.*, 102(2): 213–232

Maruyama, S., 1994. Plume Tectonics. *J. Geol. Soc. Japan*, 100: 24–49

Matyska, C., Yuen, D. A., 2006. Lower Mantle Dynamics with the Post-Perovskite Phase Change, Radiative Thermal Conductivity, Termperature and Depth-Dependent Viscosity. *Phys. Earth Planet. Inter.*, 154(2): 196–207

Matyska, C., Yuen, D. A., 2007. Lower Mantle Material Properties and Convection Models of Multiscale Plumes. In: Fougler, G. T., Jurdy, D. M., eds., Plates, Plumes and Planetary Processes. Geological Society of America Special Paper, 137–163

Mitrovica, J. X., Forte, A. M., 2004. A New Inference of Mantle Viscosity Based upon Joint Inversion of Convection and Glacial Isostatic Adjustment Data. *Earth Planet. Sci. Lett.*, 225(1–2): 177–189

Moresi, L. N., Solomatov, V. S., 1995. Numerical Investigations of 2D Convection with Extremely Large Viscosity Variations. *Phys. Fluids*, 7: 2154–2162

Nakagawa, T., Tackley, P. J., 2004. Effects of a Perovskite-Post Perovskite Phase Change near Core-Mantle Boundary in Compressible Mantle Convection. *Geophys. Res. Lett.*, 31(16): L16611

Nakagawa, T., Tackley, P. J., Deschamps, F., et al., 2010. The Influence of MORB and Harzburgite Composition on Thermo-chemical Mantle Convection in a 3-D Spherical Shell with Self-Consistently Calculated Mineral Physics. *Earth Planet. Sci. Lett.*, 296(3–4): 403–412

O'Farrell, K. A., Lowman, J. P., 2010. Emulating the Thermal Structure of Spherical Shell Convection in Plane-Layer Geometry Mantle Convection Models. *Phys. Earth Planet. Inter.*, 182(1–2): 73–84

Oganov, A. R., Ono, S., 2004. Theoretical and Experimental Evidence for a Post-Perovskite Phase of $MgSiO_3$ in Earth's D" Layer. *Nature*, 430(6998): 445–448

Oganov, A. R., Ono, S., 2005. The High Pressure Phase of Alumina and Implications for Earth's D" Layer. *Proc. Natl. Acad. Sci.*, 102(31): 10828–10831

Ohta, K., 2010. Electrical and Thermal Conductivity of the Earth's Lower Mantle: [Dissertation]. Tokyo Institute of Technology, Tokyo

Oldenbur, D. W., Brune, J. N., 1972. Ridge Transform Fault Spreading Pattern in Freezing Wax. *Science*, 178(4058): 301–304

Parmentier, E. M., 2007. The Dynamics and Convective Evolution of the Oceanic Upper Mantle. In: Schubert, G., Bercovici, D., eds., Treatise on Geophysics. Cambridge University Press, Cambridge. 7: 305–324

Poirier, J. P., 1991. Introduction to the Physics of the Earth's Interior. Cambridge University Press, Cambridge

Ricard, Y., Bai, W. M., 1991. Inferring Viscosity and the 3-D Density Structure of the Mantle from Geoid, Topography and Plate Velocities. *Geophys. J. Int.*, 105(3): 561–571

Richards, M. A., Yang, W. S., Baumgardner, J. R., et al., 2001. Role of a Low-Viscosity Zone in Stabilizing Plate Tectonics: Implications for Comparative Terrestrial Planetology. *Geochem.*, *Geophys.*, *Geosyst.*, 2(8), doi: 10.1029/2000GC000115

Richter, F., 1973. Finite Amplitude Convection through a Phase Boundary. *Geophys. J. R. Astron. Soc.*, 35(1–3): 265–276

Schenk, O., Gartner, K., Fichtner, W., 2000. Efficient Sparse LU Factorization with Left-Right Looking Strategy on Shared Memory Multiprocessors. *BIT*, 40(1): 158–176

Schubert, G., Froidevaux, C., Yuen, D. A., 1976. Oceanic Lithosphere and Asthenosphere: Thermal and Mechanical Structure. *J. Geophys. Res.*, 81(20): 3525–3540

Schubert, G., Turcotte, D. L., Olson, P., 2001. Mantle Convection in the Earth and Planets. Cambridge University Press, Cambridge. 940

Spiegelman, M., Katz, R. F., 2006. A Semi-Lagrangian Crank-Nicolson Algorithm for the Numerical Solution of Advection-Diffusion Problems. *Geochem.*, *Geophys.*, *Geosyst.*, 7: Q04014

Stein, C., Hansen, U., 2008. Plate Motions and the Viscosity Structure of the MZantle—Insights from Numerical Modelling. *Earth Planet. Sci. Lett.*, 272(1–2): 29–40

Steinbach, V., Yuen, D. A., 1995. The Effects of Temperature-Dependent Viscosity on Mantle Convection with the Two Major Phase Transitions. *Phys. Earth Planet. Inter.*, 90(1–2): 13–36

Tang, X. L., Dong, J. J., 2010. Lattice Thermal Conductivity of MgO at Conditions of Earth's Interior. *Proc. Natl. Acad. Sci. USA*, 107(10): 4539–4543

Tateno, S., Hirose, K., Sata, N., et al., 2009. Determination of Post-Perovskite Phase Transition Boundary up to 4 400 K and Implications for Thermal Structure in D" Layer. *Earth Planet. Sci. Lett.*, 277(1–2): 130–136

Tosi, N., Sabadini, R., Marotta, A. M., et al., 2005. Simultaneous Inversion for the Earth's Mantle Viscosity and Ice Mass Imbalance in Antarctica and Greenland. *J. Geophys. Res.*, 110: B07402

Tosi, N., Yuen, D. A., Cadek, O., 2010. Dynamical Consequences in the Lower Mantle with the Post-Perovskite Phase Change and Strongly Depth-Dependent Thermodynamic and Transport Properties. *Earth Planet. Sci. Lett.*, 298(1–2): 229–243

van Bemmelen, R. W., Berlage, H. P., 1934. Versuch Einer Mathematischen Behandlung Geotektonischer Bewegungen Unter Besonderer Berueecksichtigung der Undationstheorie. *Gerlands. Beitr. Z. Geophys.*, 43(1–2): 19–55 (in German)

Walte, N. P., Heidelbach, F., Miyajima, N., et al., 2009. Transformation Textures in Post-Perovskite: Understanding Mantle Flow in the D" Layer of the Earth. *Geophys. Res. Lett.*, 36: L04302

Wentzcovitch, R. M., Justo, J. F., Wu, Z., et al., 2009. Anomalous Compressibility of Ferropericlase throughout the Iron Spin Cross-over. *Proc. Natl. Acad. Sci. USA*, 106(21): 8447–8452

Wentzcovitch, R. M., Yu, Y. G., Wu, Z. Q., 2010. Thermodynamic Properties and Phase Relations in Mantle Minerals Investigated by First Priniciples Quasiharmonic Theory. *Reviews in Mineralogy and Geochemistry*, 71: 59–98

Xu, Y. S., Shankland, T. J., Linhardt, S., et al., 2004. Thermal Diffusivity and Conductivity of Olivine, Wadsleyite and Ringwoodite to 20 GPa and 1 373 K. *Phys. Earth. Planet. Inter.*, 143–144: 321–336

Yamamoto, M., Morgan, J. P., Morgan, W. J., 2007. Global Plume-Fed Asthenosphere Flow—I: Motivation and Model Development. *GSA Special Papers*, 430: 165–188

Yamazaki, D., Karato, S., 2007. Lattice Preferred Orientation of Lower Mantle Materials and Seismic Anisotropy in the D" Layer. In: Hirose, K., Brodholt, J., Lay, T., et al., eds.,

Post-Perovskite: The Last Mantle Phase Transition. *AGU Monograph*, 174: 69–78

Yoshino, T., Yamazaki, D., 2007. Grain Growth Kinetics of $CaIrO_3$ Perovskite and Post-Perovskite, with Implications for Rheology of D" Layer. *Earth Planet. Sci. Lett.*, 255(3–4): 485–493

Yu, Y., Wu, Z., Wentzcovitch, R. M., 2008. α-β-γ Transformations in Mg_2SiO_4 in Earth's Transition Zone. *Earth Planet. Sci. Lett.*, 273: 115–122

Yuen, D. A., Cadek, O., van Keken, P., et al., 1996. Combined Results from Mineral Physics, Tomography and Mantle Convection and Their Implications on Global Geodynamics. In: Boschi, E., Morelli, A., Ekstrom, G., eds., Seismic Modelling of the Earth's Structure. Editrice Compositori, Bologna. 463–505